

An integrated resource-efficient microfluidic device for parallelised studies of immobilised chiral catalysts in continuous flow via miniaturized LC/MS-Analysis

Hannes Westphal,^{a†} Rico Warias,^{a†} Chris Weise,^a Daniele Ragno,^b Holger Becker,^c Matthias Spanka,^d Alessandro Massi,^b Roger Gläser,^c Christoph Schneider,^d Detlev Belder^{a*}

^aLeipzig University, Institute of Analytical Chemistry, Linnéstraße 3, 04103, Germany

E-mail: belder@uni-leipzig.de

^bUniversity of Ferrara, Department of Chemical, Pharmaceutical and Agricultural Sciences,
Via L. Borsari 46, 44121, Italy

^cLeipzig University, Institute of Chemical Technology, Linnéstraße 3, 04103, Germany

^dLeipzig University, Institute of Organic Chemistry, Johannisallee 28, 04103, Germany

† These authors contributed equally to this manuscript.

Abstract: A highly integrated microfluidic device is presented for the parallelised study of stereoselective heterogeneous catalytic processes. For the first time, multiple packed-bed μ -flow reactors are combined with a chiral separation unit on a chip that is seamlessly connected to mass spectrometry. By developing an automated fluidic setup, this device allows the performance of different catalysts to be studied in a single run, using only small amounts of resources. In this way, fully automated quasi-simultaneous testing of 2-packed bed reactors for enantioselectivity and conversion is possible, with a significant reduction in solvent and substrate consumption compared to classical tube reactor HPLC-MS testing.

1. Microchip fabrication and modification
 - a. Chip layout
 - b. Microchip fabrication
 - c. Chip modification
2. Instrumental setup
 - a. Valving and schematics
 - b. Coupling with mass spectrometry
 - c. Automation of the injection principle
3. Additional information on performed experiments and applications
 - a. Evaluation of the injection principle and compatible solvents
 - b. Other waterfall chromatograms for solvent screening
 - c. Long-term evaluation – additional information
 - d. 2R – PS/Si comparison in single chip
4. Continuous flow model reactions and peak identification
5. Syntheses and immobilization of the organocatalysts
6. References

1. Microchip fabrication and modification

1.1. Chip layout

The chip design of the presented multi-reactor device consists of two mirrored reactor channels and one separation column, each connected to a packing channel for slurry packing. The respectively used photomask for manufacturing, as well as a manufactured and fully prepared microchip are depicted in Fig. S01. Both reactor channels had a length of approximately 95 mm and a width of 100 μm . The channel depths were approximately 35 μm , resulting in an estimated reactor volume of approximately 150 nl for each packed reactor (assuming an exclusion volume of 50% for the packed reactor). The separation channel had a length of 60 mm and a width of 50 μm . In addition to the two reactors and the separation column, there are constrictions (positions 1, 2, and 3 in Fig. S01 A) for anchoring photopolymerized porous frits to immobilize the packed material. Those constrictions have a width of 25 μm on each side of the separation column and 40 μm for the reactor channel. Furthermore, the microfluidic chip contains powder-blasted holes for fluidic contact, utilized to connect the chip to the outer periphery by a homemade steel clamp system.

The initial chip design contained an additional sheat flow channel after the separation column, which was removed during the grinding of the emitter tip for the coupling with nano-ESI-MS. However, if the on-chip separation would be operated as normal phase chromatography instead, the sheat channel could be maintained to enable a stable electrospray by the addition of an aqueous fraction after the separation column.

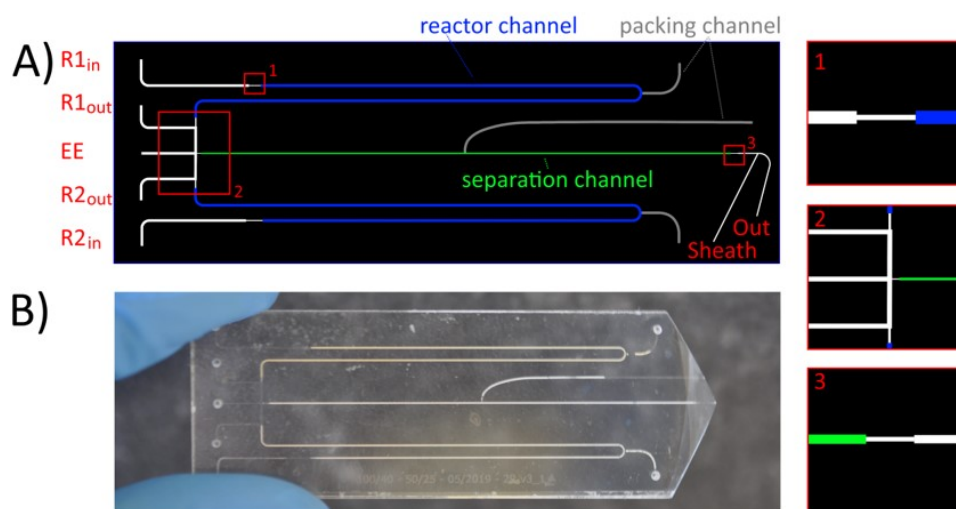


Fig. S01 Scheme of the used photomask for manufacturing and explanation of the functional units included in the microfluidic device with two reactors. Furthermore, a photography of the fully prepared chip is depicted. **A)** left: The mask shown was used in the manufacturing process's lithographic step, and the functional units are visualized in different colors. Additionally, the chip inlets and outlets are marked. For a better visibility, the channel dimensions are tripled in this illustration; right: Magnified views of the marked areas (1. Constriction at the first reactor, 2. Injection cross, 3. Constriction after separation column); **B)** Photo of the manufactured and fully modified microchip.

1.2. Microchip fabrication

The whole fabrication process for the microfluidic device is illustrated in Fig. S02 and explained briefly in the following. For fabrication, soda lime glass slides (**1**; approx. 76 x 26 x 1 mm) with a 150 nm thick sputtered chrome layer (**2**; sputtered by FHR Anlagenbau GmbH, Ottendorf-Okrilla, DE) were used. The sputtered metal layer was applied to increase the substrate's resistance for the later wet etching process. The glass slides were first cleaned with acetone and iPrOH, then a positive photoresist (AZ 1518, MicroChemicals GmbH, DE) was applied by spin coating (**3**; 4000 rpm, 1000 rpm/s, 30 s). The

photoresist layer was soft-baked by heating the slides for 5 min at 110 °C, followed by 2 min at 90 °C and 2 min at 70 °C. The photomasks were then positioned on top of the photoresist and irradiated with UV light (**4**; 14 mJ/cm², 30 s). After irradiation, the positive resist was processed in a developer bath (**5**; AZ 351B:H₂O, 1:4, v/v, MicroChemicals GmbH, DE) for 80 s, during which the previously illuminated sections were dissolved and then removed to obtain the desired mask template. The underlying exposed chromium layer was dissolved in chromium etch for 1 min (**6**; TechniStrip Cr01, MicroChemicals GmbH, DE). Then, the substrate was placed for wet chemical etching in a bath of buffered hydrogen fluoride solution (**7**; HF:NH₄F = 12.5:87.5%, BOE 7:1, MicroChemicals GmbH, DE) for 50 min. Subsequently, the photoresist was removed with acetone, and the remaining sputtering chrome with the chromium etch (**8**). Afterward, holes were powder-blasted as an inlet or outlet in a second glass slide, and the two glass slides were merged by high-temperature fusion bonding (**9**). For this process, the glass slides were cleaned with EtOH and heated at 150 °C for 1 h in a solution of H₂O, NH₃, and H₂O₂ (3:2:1, v/v/v) to activate the glass surface. Then, the etched glass slides were aligned with the powder blasted glass slides as lids and placed in an oven. In the applied temperature program, they were first heated to 500 °C in 50 min, then the temperature was kept constant for 15 min, then increased to 550 °C in 15 min and kept constant for 30 min. After that, the temperature was increased to 620 °C within 15 min and kept constant for 180 min. Finally, the temperature was cooled down to RT within 600 min.

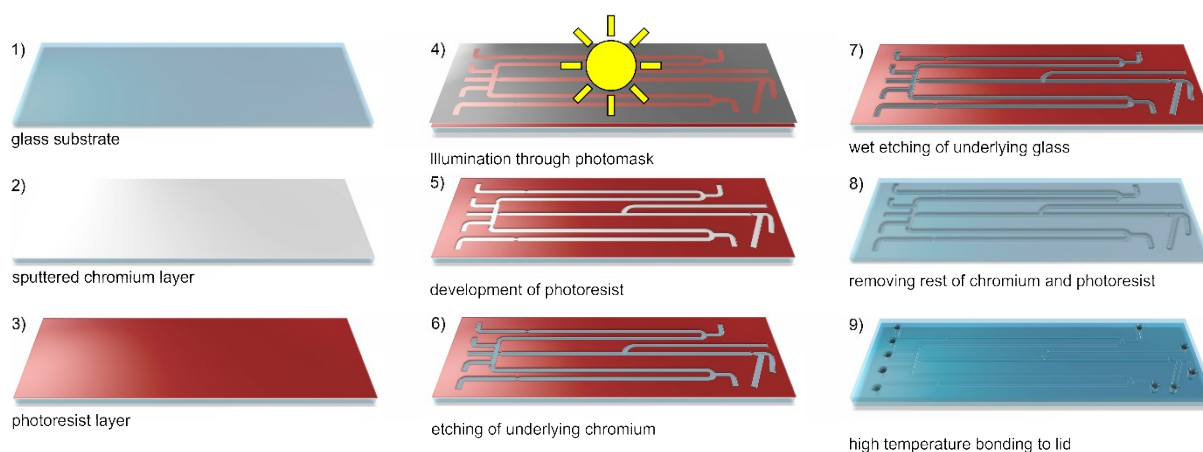


Fig. S02 Preparative steps for chip manufacturing. **1)** Soda-lime glass as substrate, **2)** sputtering of the glass surface with a thin chromium layer, **3)** Application and baking of a thin layer of photoresist, **4)** Light exposure through printed foil photomask, **5)** Processing of the photoresist in a developing bath, **6)** Chromium etching, **7)** Wet chemical etching of the glass using HF, **8)** Removal of the photoresist and chromium layer, **9)** Thermal fusion bonding with another glass slide including powder-blasted inlets.

1.3. Chip modification

After manufacturing (Fig. S03 A), the chip device was further modified to allow the integration of packed reactors and separation channels as well as a monolithic electrospray emitter. Since the respective steps were described in detail elsewhere,^[1] only a short summary is given here. At first, photopolymerized porous frits were integrated as particle retaining elements, as shown in Fig. S03 B (in total 6 porous frits, integrated before and after reactor and separation channels). The composition of the pre-polymer solution for the frits is listed in Fig. S04 B. Subsequently, the reactor and separation columns were filled by slurry packing through a designated packing channel for each column (Fig. S03 C). Afterwards the packing channels were sealed by integrating photopolymerized plugs, as shown in Fig. S03 D (in total 3 plugs, at the end of each packing channel). The composition of the pre-polymer solution for the plugs is listed in Fig. S04 C. Then, a monolithic electrospray emitter was grinded after the separation channel (Fig. S03 E). Finally, the emitter was hydrophobized by an in-house protocol to minimize the accumulation of liquid at the emitter tip as described in Fig. S04 D.




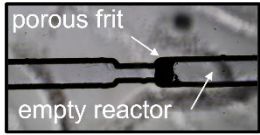
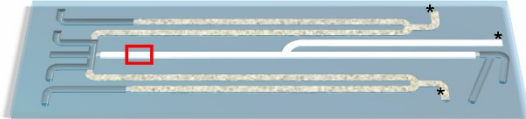
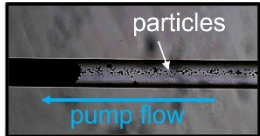
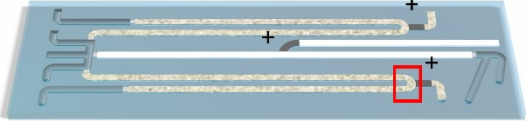
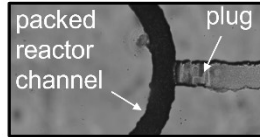
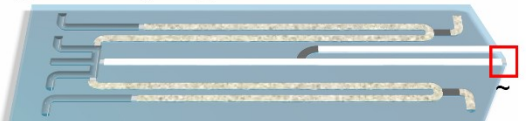
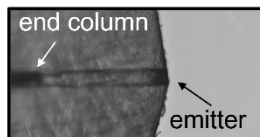
#	Chip modification after manufacturing	
A) Step 1 Evaluation of the manufactured chip	<ul style="list-style-type: none"> - positions of fluidic inlets  	<ul style="list-style-type: none"> • After chip fabrication, all channels are first examined for potential etching imperfections. • Then fluidic permeability is tested by connection to a syringe pump to the different inlets.
B) Step 2 Photopolym. of porous frits	<ul style="list-style-type: none"> o positions of photopolymerized porous frits  	<ul style="list-style-type: none"> • Integration of photopolymerized porous frits as particle retaining elements at the end of each separation and reactor channel (local irradiation by using a focused 365 nm LED). • Introducing the pre-polymer solution by a syringe through one of the inlets.
C) Step 3 Packing of the separation & reaction channels	<ul style="list-style-type: none"> * positions of packing channel inlets  	<ul style="list-style-type: none"> • Slurry packing of the separation and reactor channels through packing channels. • Pumping of slurry ($2\text{-}5\text{ mg}\cdot\text{mL}^{-1}$ in MeCN) by an HPLC pump ($3\text{-}20\text{ }\mu\text{L}\cdot\text{min}^{-1}$, 100-130 bar)
D) Step 4 Photopolym. of plugs	<ul style="list-style-type: none"> + positions of photopolymerized unporous plugs  	<ul style="list-style-type: none"> • Closing the packing channels by photopolymerization of unporous plugs (at the end of each packing channel by local irradiation using a focused 365 nm LED) • Introduction of the pre-polymer solution with an HPLC pump through one of the inlets.
E) Step 5 Grinding the ESI-emitter tip	<ul style="list-style-type: none"> ~ position of the grinded pyramidal nanoESI-emitter  	<ul style="list-style-type: none"> • Grinding of a monolithic nano-ESI emitter, by sawing the end of the chip with a dremel and subsequently grind the tip to form a pyramidal emitter. • Afterwards hydrophobization of the emitter by an in-house protocol.

Fig. S03. Detailed description of the different modification steps performed on the manufactured microfluidic chips.

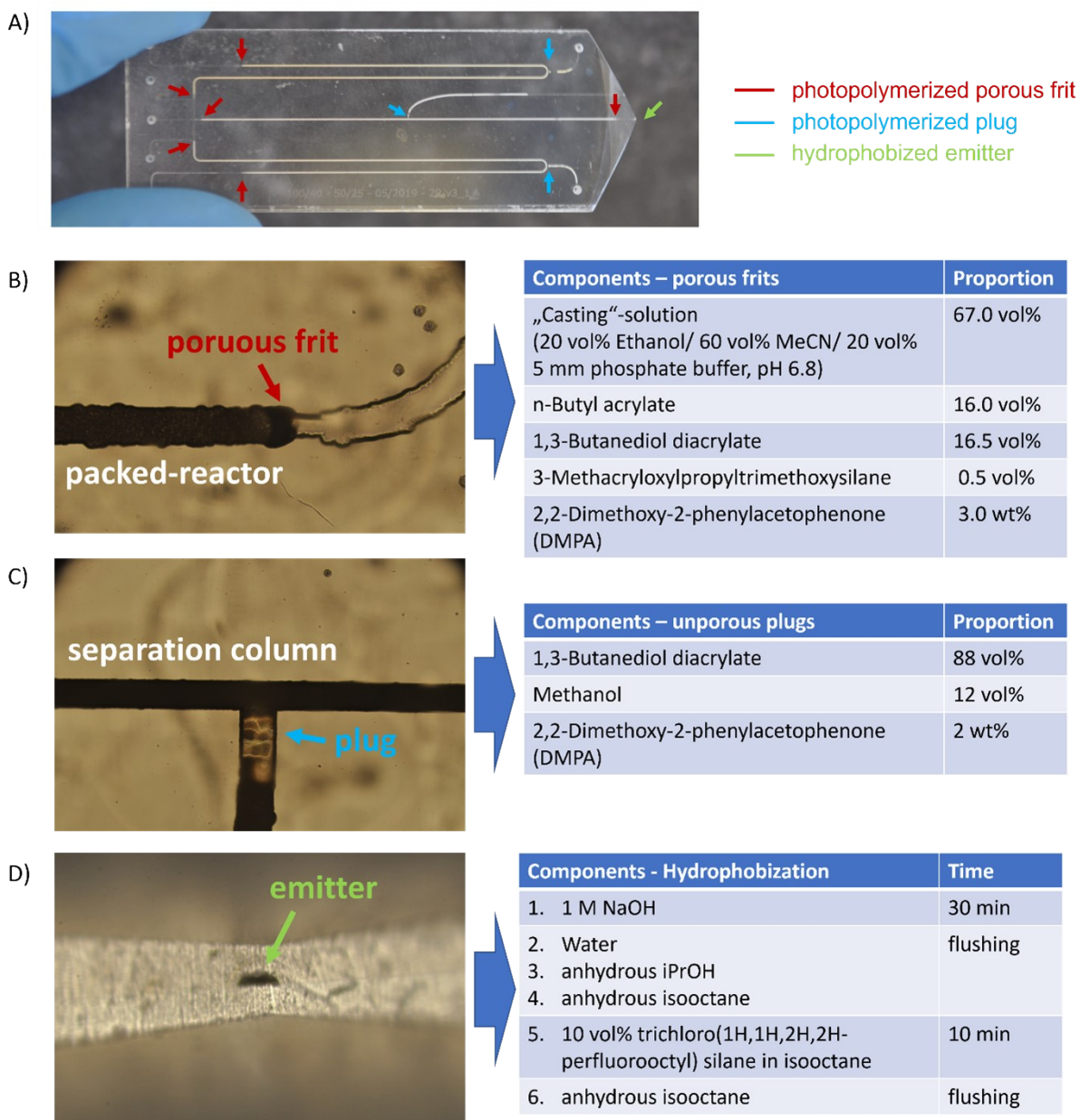


Fig. S04 **A)** Positions of different chip modifications & composition of the pre-polymer solutions and for hydrophobization. The plugs and frits are introduced by photopolymerization by irradiation with a focused 365 nm LED, using a modified inverted epi-fluorescence microscope. **B)** Picture of one integrated porous frit, which is utilized as a particle retaining element at the ends of each column. Furthermore, all pre-polymer solution components are listed. **C)** Picture of an integrated plug, which seals the packing channels after slurry-packing. Additionally, the composition of the corresponding pre-polymer solution is listed. **D)** Hydrophobization of the grinded electrospray emitter tip by an in-house protocol.

2. Instrumental setup

2.1. Valving and schematic

In the following section, all connections of the instrumental fluidic setup are described in detail. Subsequently, the respective valving to realize the injection principle is illustrated and briefly explained. First, the corresponding lengths of the capillary tubings in the instrumental setup are illustrated in Fig. S05. The main fluidic circuit was constructed by four electrically actuated nanovolume valves (10-port, 100 μm bore, Cheminert, VICI AG, Schenkon, Switzerland). All connections were made using commercially available PEEK capillary tubings (50 and 100 μm ID, 360 μm or 1/16" OD) and PEEK connections such as screws, ferrules, crosses, plugs, and other fittings (primarily Nanovolume fittings for 360 μm OD, Cheminert, ViciJour). Further inline filters (2 μm , SS frit, JR-0611-SS2-3, VICI AG International, CHE) were applied after the pump outlets as well as after sample syringes to avoid contamination by particles. Additional filters (1 μm SS frit, M-133/M-543, IDEX Corporation, USA) were positioned after the chip outlets to avoid clogging or damaging the subsequent Nanovolume valves by loose column material. For the fluidic contact, a homemade steel clamp system was utilized to connect the chip with the outer periphery.^[2] Two identical isocratic pumps applied the flow through the two reactor channels (LC-20AD, Shimadzu, Kyoto, Japan). For the elution flow, a modulated 1260 Infinity HPLC-system (Agilent, Santa Clara, US) was utilized, including an isocratic pump for the pinch flow and a binary pump for the eluent flow.

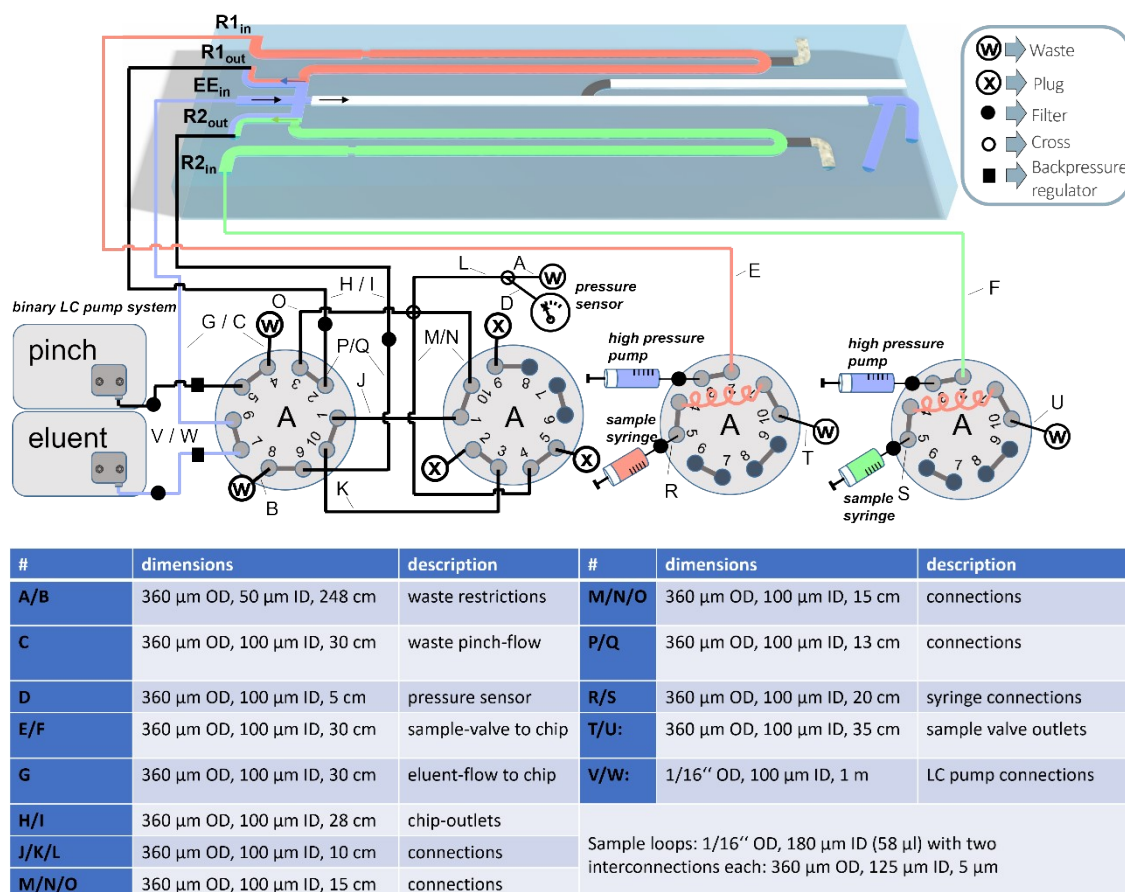


Fig. S05. Detailed picture of the instrumental setup suitable for the operation of a microfluidic chip with two continuous flow reactors, including all necessary components and capillary tubing length information.

Generally, the injection sequence is based on the control of four electrically actuated Nanovolume valves. To emphasize the injection principle, different steps of the corresponding injection sequence are exemplarily shown in Fig. S06 1-3) and explained briefly in the following section.

The first valve enables switching between elution and injection mode. During elution mode (valve 1 in A position; Fig. S06 1), the flow from the eluent (**EE_{in}**) is mainly present in the injection cross, while both reactor effluents continuously enter the bypass channels (**R1/2_{out}**), which were connected to a joint restriction and finally to the waste outlet. By switching into injection mode for the first reactor (valve 1 in B position; Fig. S06 2), only the bypass channel of that reactor (**R1_{out}**) is blocked so that the flow of the reactor is directed to the injection cross and then, together with the effluent of the second reactor, into the bypass channel of the second reactor outlet (**R2_{out}**). To support this, the "elution"-flow is switched to a "pinch"-flow with decreased flow rate (**EE_{in}**). During this injection process, part of the reactor effluent is loaded at the HPLC column head and can be injected and eluted by switching back to elution mode (Fig. S06 1).

The second valve is now used to enable injection of the second reactor instead (valve 1 in B position; Fig. S06 3). In this position, the second reactor bypass outlet (**R2_{out}**) is blocked during injection-mode so that the effluent of that reactor is directed to the injection cross, accumulating at the column head, and finally flows together with the first reactor effluent in the first bypass outlet (**R1_{out}**). Then, the sample plug at the column head can be eluted again by switching back to the elution mode (valve 1 in A position, Fig. S06 1).

The third and fourth valves contain large sample loops, which enable the loading of new reaction mixtures (Valve 3 or 4 in position A) by using glass syringes (Hamilton, CHE). The reactants can then be flushed onto the packed reactor for continuous operation (Valve 3 or 4 in position B).

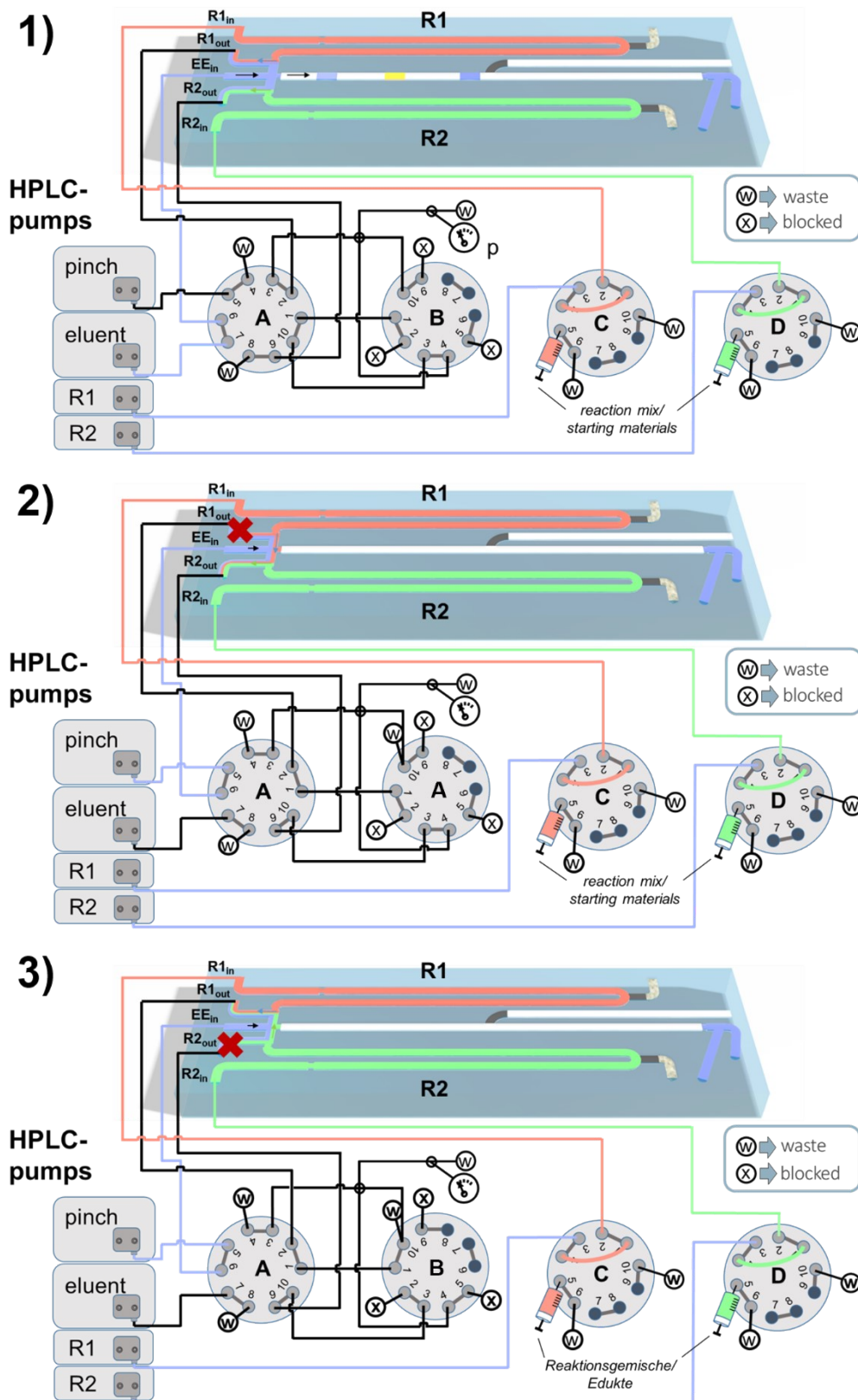


Fig. S06 Schematic of the instrumental setup to operate a microfluidic chip with two integrated flow reactors; **R1-2_{in}**: Reactor inlets, **R1-2_{out}**: Reactor outlets; **EE_{in}**: Inlet for the elution or pinch pump stream, **w**: Waste outlet, **x**: sealed connection. 1) During elution mode both reactors run continuously in bypass channels, while injected samples can be eluted along the separation column. 2) Injection of a sample plug from the first reactor. 3) Injection of a sample plug from the second reactor.

2.2. Coupling with mass spectrometry

The microfluidic chips were hyphenated to a quadrupole ion trap mass spectrometer (AmaZon SL, Bruker Daltonik GmbH, Bremen, DE) for detection after the on-chip separation column (as shown in Fig. S07 A). A custom metal stage was used for coupling the chip, which can be hung onto the MS inlet and enables stabilization of the connected valves. The chip was placed on the stage on top of a three-axis miniature linear translational stage (T12XYZ/M and T12B, Thorlabs, New Jersey, USA) for positioning in front of the MS inlet (see Fig. S07 B). Depending on the flow rate and the composition of the mobile phase, the distance between the chip emitter and the spray shield was adjusted (approx. 2-3 mm). During electrospray operation, the transfer capillary voltage was set to 4500 V and the offset endplate to 500 V, while the chip was grounded via fluidic contact to the connected HPLC-pumps. The mass spectrometer was operated in positive and enhanced resolution mode with a scan range of 50-800 m/z at an acquisition rate of approximately 3 spectra·s⁻¹. Additionally, the dry gas flow was set to 4 L·min⁻¹ at a temperature of 300-350 °C.

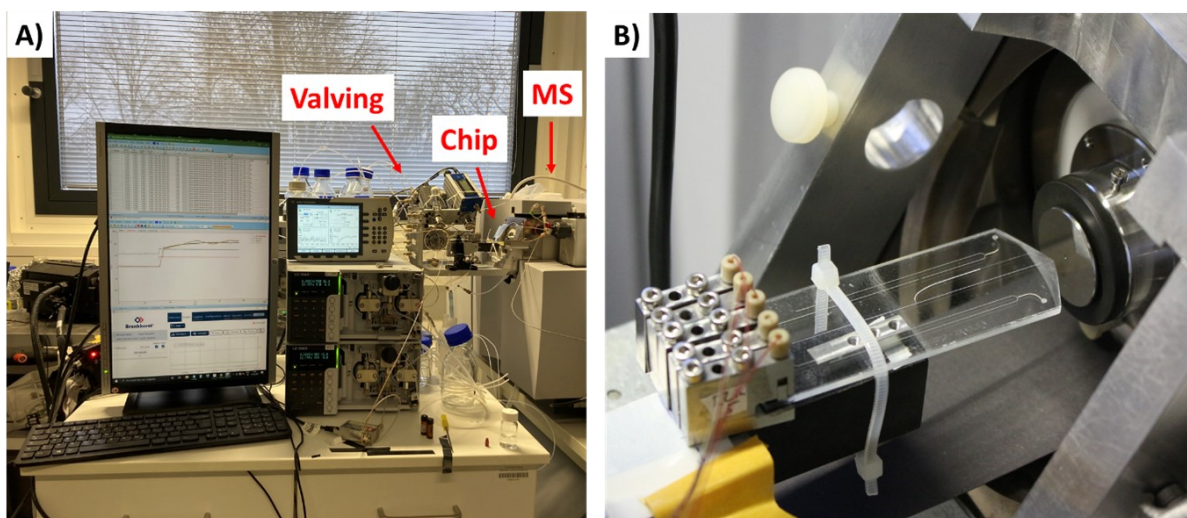


Fig. S07 Photography of the instrumental setup in front of the mass spectrometry; **A)** The picture shows the respective pumps as well as the custom metal stage which enables stabilization of the connected valves and positioning of the microfluidic device; **B)** Microfluidic chip positioned in front of the MS inlet with a three-axis miniature linear translational stage. The fluidic connection of the chip was realized by a custom steel clamp system.

2.3. Automation of the injection principle

For automatization of the injection principle, a "Clarity chromatography data station" was utilized in combination with a "Colibrick" A/D converter box (DataApex, Prague, CZ), whereby all respective connections are displayed in Fig. S08. The box contains 4 channels for analogue data logging, which were used for pressure monitoring of the pumps as well as an external pressure sensor, which was connected at one of the reactor bypass outlets (R1_{out}). Furthermore, the box contains 4 digital outputs (TTL, 5 V), which were used to start/stop the MS-acquisition by addressing the I/O-pins of the mass spectrometer, triggering the box itself to start the next acquisition, or stopping all pumps at the end of the run or if leakage occurs (triggered by a pressure drop at the external pressure sensor). Then, the box contains 4 digital inputs (TTL, 5 V), which were mainly not used, except for one to trigger the box itself to start the next acquisition, as said before for one of the digital outputs (IN 1 as an external start, closed connection, "down" here as default).

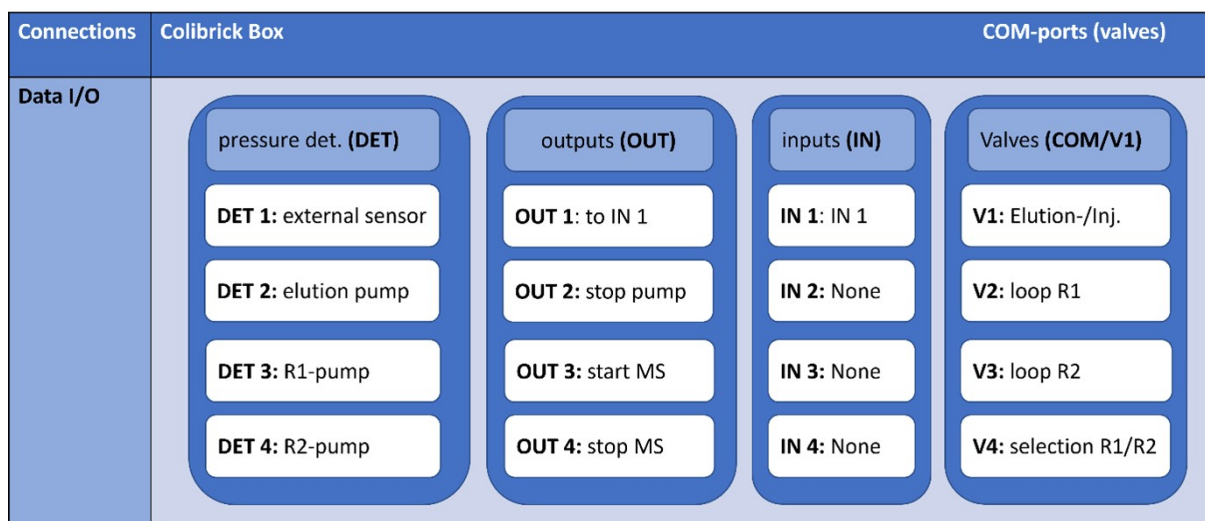


Fig. S08 Illustration featuring the I/O-connections and detection channels for pressure monitoring. For most serial connections a "Colibrick" A/D converter box was utilized in combination with a Clarity chromatography data station (DataApex, Prague, CZ). The valves were connected via USB and addressed through the respective COMports.

The four electrically actuated Nanovolume valves (Cheminert, VICI AG, Schenkon, Switzerland) were connected via a serial-to-USB converter to enable control with the clarity software as well. For running multiple acquisitions in sequence, different methods were written in the Clarity software, as shown in Fig. S09. The different method blocks can be repeated or alternated as many times as requested, only limited by the choice of the size of the sample loop as a sample reservoir.

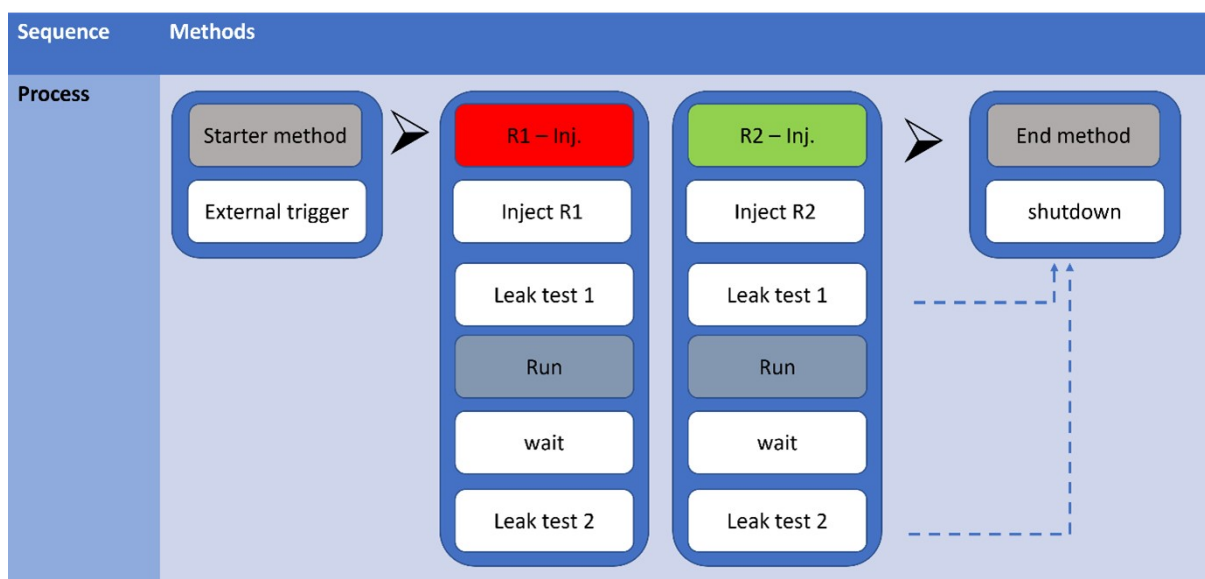


Fig. S09 Schematic featuring the automatized injection sequence to perform multiple automatized consecutive or alternating acquisitions. The method blocks can be repeated as many times as requested for the run.

The different functions, included in the method blocks are explained in detail in Fig. S10. The first method is a starter method, which is started by an external trigger (OUT 1 to IN 1; external start through a switch to open connection, "up"). During this method, the sample loop valves can be switched onto the reactor stream (which could be integrated into the method but was mostly done manually) and the reactor can be subsequently flushed at increased flow rate, before the start of the first injection. As soon as the external trigger is started, the next method block starts, which is the first acquisition. All subsequent acquisitions are executed one by one in a method sequence table and start as soon they are loaded (external start IN 1 through closed connection, "down", as set as default). In the first step of the acquisition method, the corresponding reactor is sampled onto the separation column by the respected valving (as visualized more detailed in the next section), and the MS-acquisition is started (OUT 3). The pressure drops temporarily during the injection mode and then increases again as soon as the system

switches back to elution mode. If the pressure does not rise again after injection due to a leak, a protection mechanism is triggered ("Leak detection 1"), which turns off all pumps and stops all ongoing measurements by jumping to the "End" method. If, on the other hand, the pressure rises again and thus the injection works, a switch is made to a "Run" method. This method is executed as long as the separation time is set and finally terminates the MS-acquisition. Furthermore, if the pressure at the chip outlet drops during this method below a certain limit due to a leakage, a second protection mechanism is triggered ("Leak detection 2"), which also shuts down the system. Then, if all acquisitions in the sequence table are carried out, the system also switches to the "End" method to turn off all connected pumps.

Methods	Function modules
Starter method	<div style="border: 1px solid black; padding: 5px; margin-bottom: 5px;"> External trigger <ul style="list-style-type: none"> Start method only if external trigger is applied (IN 1) </div>
R1 – Inj.	<div style="border: 1px solid black; padding: 5px; margin-bottom: 5px;"> Inject R1/R2 <ul style="list-style-type: none"> Start MS at t=0 min (OUT 3) Switch to the reactor that should be injected (R1: pos 1, R2: pos 2) Injection mode Valve 1 (pos 2) at t = 0.2 min Elution mode Valve 1 (pos 1) at t = 0.2 min + inj.-time </div> <div style="border: 1px solid black; padding: 5px;"> Leak test 1 <ul style="list-style-type: none"> Switch to "Run" method if injection works (external pressure sensor (DET 1) > 30 bar after injection) Jump to End-method if leakage occurs during injection </div>
R2 – Inj.	
Run	<div style="border: 1px solid black; padding: 5px;"> wait <ul style="list-style-type: none"> Wait for the time that the separation lasts Then stop MS-acquisition (OUT 4) </div>
End method	<div style="border: 1px solid black; padding: 5px; margin-bottom: 5px;"> Leak test 2 <ul style="list-style-type: none"> switch to „End“ method if leakage occurs (external sensor (DET 1) < 10 bar during separation) </div>
	<div style="border: 1px solid black; padding: 5px;"> shutdown <ul style="list-style-type: none"> Turn off all pumps (OUT 2) Then stop MS-acquisition (OUT 4, if a leakage test triggered) </div>

Fig. S10 Explanation of the different function modules that are integrated into the method blocks of Fig. S09.

3. Additional information on performed experiments and applications

3.1. Evaluation of the injection principle and compatible solvents

The injection principle to perform an independent injection from both integrated reactors was evaluated by injecting fluorescent dyes (R1: coumarin 120, 100 $\mu\text{g}\cdot\text{ml}^{-1}$ in MeCN; R2: fluoranthene, 200 $\mu\text{g}\cdot\text{ml}^{-1}$ in MeCN) into the two respective reactor streams. Subsequently, the streams were illuminated by a mercury vapor lamp and observed with an epi-fluorescence microscope as depicted in Fig. S11 A&B. A bandpass filter (350/50 nm) was used for this purpose. Then, the light was guided through a long-pass filter (> 390 nm) and finally a dichroic filter (380 nm) before observation. Thereby, the injection principle proved to be stable for reactor flow rates tested from 0.5 to 1 $\mu\text{l}\cdot\text{min}^{-1}$ in combination with an elution flow rate from 75-100 $\mu\text{l}\cdot\text{min}^{-1}$ for an eluent composition of MeCN:H₂O ranging from 90:10 to 45:55. Furthermore, the applicability of the injection principle was tested for different solvents and flow parameters, as listed in Fig. S11 C. Thereby, it was for instance possible to use MeOH and MeCN

without any limitations, or it was also possible to even use two different solvents in each reactor. For EtOH, the injection principle became slightly unstable for an increased reactor flow rate of $1 \mu\text{l}\cdot\text{min}^{-1}$ for an eluent composition of 50:50 vol% (MeCN:H₂O). For more apolar solvents such as dioxan or DMSO an operation at increased reactor flow rate proved to be difficult due to the resulting increased pressure during operation or mixing problems. Therefore, the reactor flow rates were adjusted according to the respective viscosity to enable an operation with DMSO. An operation with chlorinated solvents such as DCM or CHCl₃ was generally possible, even though the mixing behavior with the eluent solvent was not optimal.

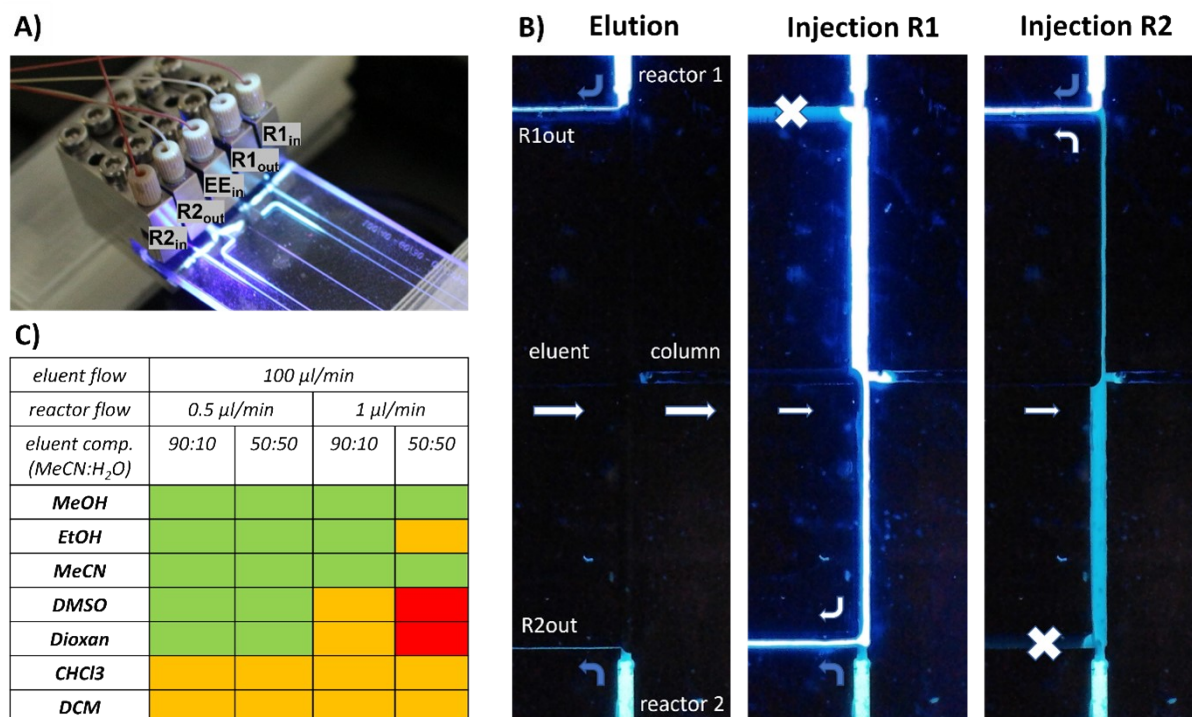


Fig. S11 Visualization of the injection principle for both reactors and verification for different reactor flow rates and eluent compositions tested; **A)** Illumination of the chip after introduction of fluorescent dyes to the corresponding reactor channels (coumarin 120 in R1, $100 \mu\text{g}\cdot\text{ml}^{-1}$ in MeCN; fluoranthene in R2, $200 \mu\text{g}\cdot\text{ml}^{-1}$ in MeCN); **B)** Visualization of the different streams of the reactor effluents during elution mode and the individual injection modes for both reactors. Fluorescent dyes were used to visualize the individual injections from each reactor; Reactor: Blank Kromasil 60 Å, 5 μm , with a flow rate of $1 \mu\text{l}\cdot\text{min}^{-1}$ (60-90 bar backpressure). Column: Chiralpak IG-3. Mobile phase: $75 \mu\text{l}\cdot\text{min}^{-1}$, H₂O:MeCN (50:50 vol% with 0.1 vol% FA; 40 bar at injection cross). Pinch flow: $2 \mu\text{l}\cdot\text{min}^{-1}$, H₂O:MeCN (50:50 vol% with 0.1 vol% FA); **C)** Evaluation of the injection principle and continuous operation for the two reactors for different solvents tested. A fully stable functionality is marked in green, while a non-optimal, but still functional operation (elevated pressures or less stable) is marked in orange. An unstable operation is marked in red.

3.2. Other waterfall chromatograms for solvent screening

In the first application, both reactors were operated simultaneously with different reactions running in each reactor. Thereby, an α -amination was performed in the first reactor with a TBS-protected immobilized Jørgensen-Hayashi catalyst (\varnothing 5 μm silica; estimated loading $f = 0.38 \text{ mmol}\cdot\text{g}^{-1}$), while a Mannich-reaction was conducted in the second reactor on an immobilized Ley-Arvidsson-Yamamoto catalyst (\varnothing 5 μm silica; estimated loading $f = 0.76 \text{ mmol}\cdot\text{g}^{-1}$). For these experiments, both catalysts used were immobilized on a silica support. In the first experiment, both reactors were operated with MeCN as solvent and sampled alternately approximately each 20 min as shown in Fig. S12 a&b. Subsequently, an experiment was conducted in which DMSO was used as a solvent in the first reactor and DCM in the second reactor (Fig. S12 c&f). Finally, the experiment was repeated using DCM in the first reactor and DMSO in the second reactor (Fig. S12 d&e). In comparison to the figure in the manuscript, all experiments are shown with multiple chromatograms as waterfall diagrams in Fig. S12.

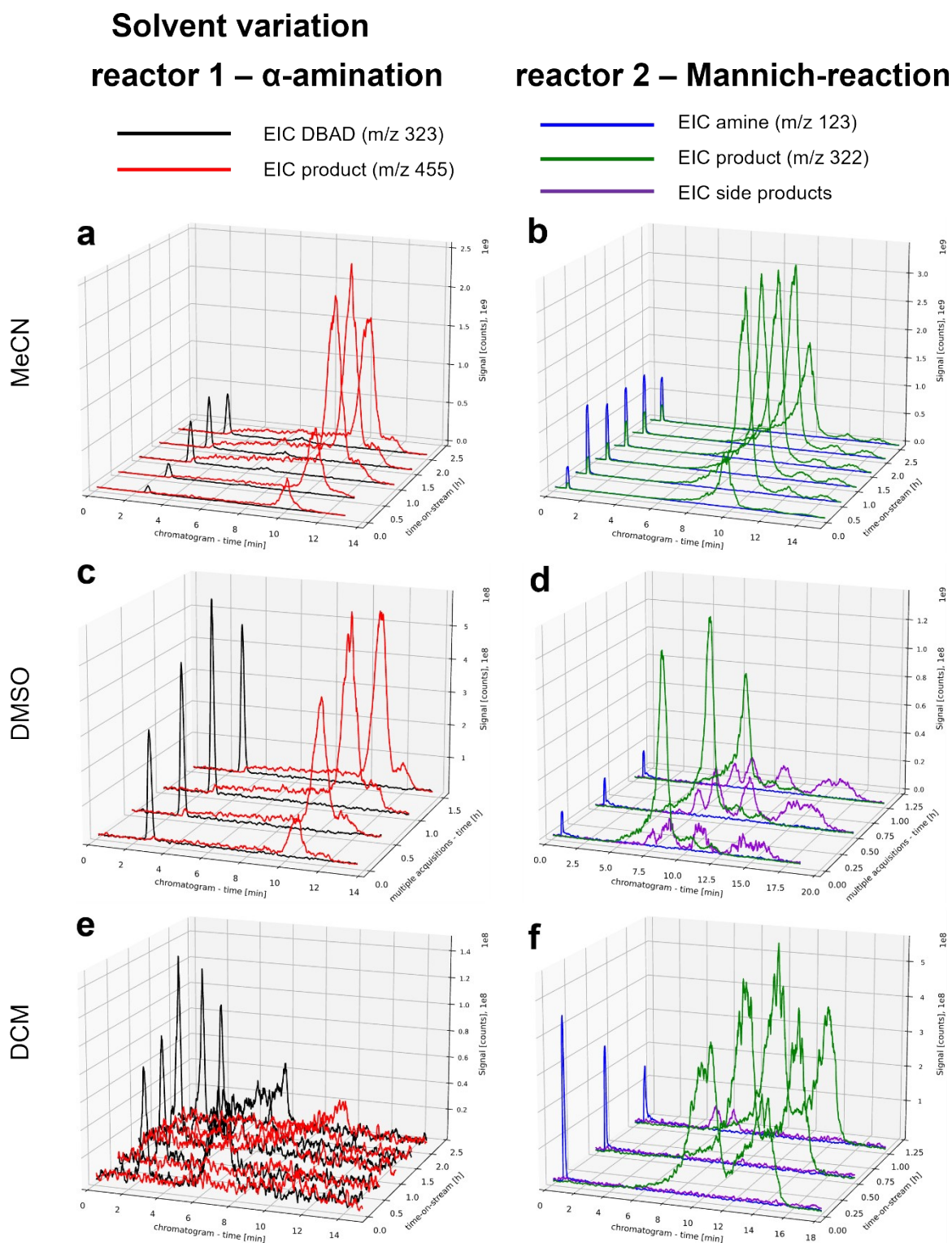


Fig. S12 Comparison of the sample solvent influence on both reactions. Two connected experiments were conducted parallel in a single microfluidic device with alternate sampling. Reactor 1 (R1): packed with TBS-HJ (\emptyset 5 μm silica; estimated loading $f = 0.38 \text{ mmol}\cdot\text{g}^{-1}$); reactor 2 (R2): packed with Lay-Cat. (\emptyset 5 μm ; loading $f = 0.76 \text{ mmol}\cdot\text{g}^{-1}$). EICs shown of the respective products and the starting materials DBAD, as well as the corresponding amine. The data was smoothed by rolling averages (sum=15). Column: Chiralpak IG-3, 3 μm , mobile phase: 100 $\mu\text{l}\cdot\text{min}^{-1}$, $\text{H}_2\text{O}:\text{MeCN}$ (55:45 vol% with 0.1 vol% FA; 52 bar at injection cross), with a linear flow of 1.6 $\text{mm}\cdot\text{s}^{-1}$ across the column. Pinch flow: 2 $\mu\text{l}\cdot\text{min}^{-1}$, $\text{H}_2\text{O}:\text{MeCN}$ (50:50 vol% with 0.1 vol% FA); **a&b**) In MeCN, reactor runtime R1: 94 min, R2: 96 min, sample flow 1 $\mu\text{l}\cdot\text{min}^{-1}$ (60-70 bar; 9 s residence time) each reactor. Injection time was 2 s each. **c&d**) In DMSO, reactor runtime R1: 94 min, R2: 96 min, sample flow R1: 0.8 $\mu\text{l}\cdot\text{min}^{-1}$ (101 bar, 14 s residence time), R2: 0.5 $\mu\text{l}\cdot\text{min}^{-1}$ (114 bar, 18 s residence time). Injection time was 3 s each. **e&f**) In DCM, reactor runtime R1: 125 min, R2: 108 min, sample flow R1: 1 $\mu\text{l}\cdot\text{min}^{-1}$ (93 bar; 9 s residence time), R2: 1 $\mu\text{l}\cdot\text{min}^{-1}$ in DCM (84 bar, 9 s residence time). Injection time R1: 5 s, R2: 3 s.

3.3. Long-term evaluation – additional information

For long-term stability investigations of the system, the injection principle and data acquisition were automatized by using a "Clarity" chromatography data station in combination with a "Colibrick" A/D-converter box (DataApex, Prague, CZ), as explained in detail in section 2.3. Then, the same microfluidic chip as in the previous section was utilized for long-term observation with alternating injections each 25 min for around 16 h in total ($n_{\text{total}} = 39$). For visualization of the system's stability, the chromatographic retention times for the reactants and products of both investigated reactions are depicted in Fig. S13 A. Thereby, a slight trend of these retention times can be observed, which can be connected to a slight increase of the measured pump pressures as illustrated in Fig. S13 B. A combined trend of all pump pressures results from the fact that all three pumps meet each other in the injection cross, and for that reason, an increase in one pump pressure results in an increase of the other ones too. Nevertheless, these changes could result from slowly reaching a pump equilibration of the applied low flow rates, or by changes in the permeability of the packed reactors by time.

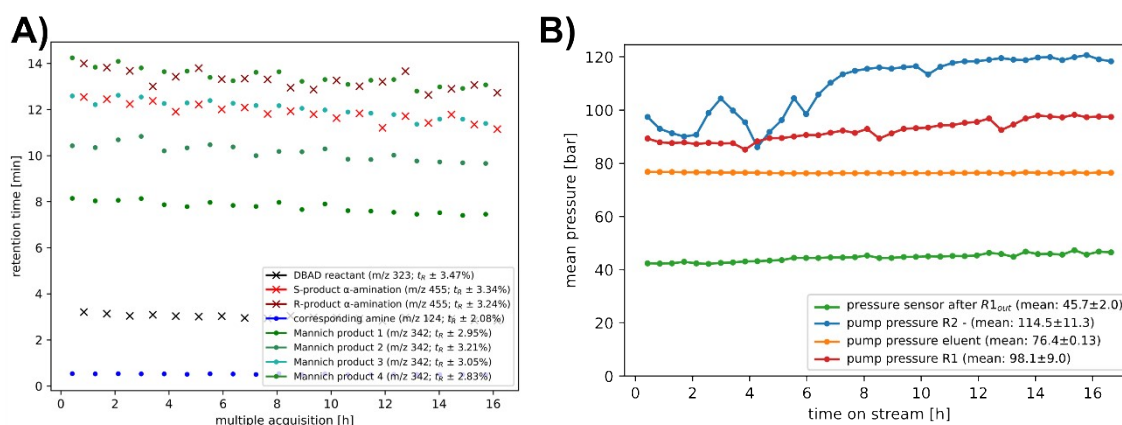


Fig. S13 A) Evaluation of the system stability while performing alternating injections during extended runtime ($n=39$) through visualization of the corresponding retention times (for α -amination shown as crosses, for Mannich-reaction shown as dots); Reactor 1 (R1): packed with TBS-HJ (ϕ 5 μm silica; estimated loading $f = 0.38 \text{ mmol}\cdot\text{g}^{-1}$); reactor 2 (R2): packed with Lay-Cat (ϕ 5 μm ; loading $f = 0.76 \text{ mmol}\cdot\text{g}^{-1}$). Reactor flow rate: 0.5 $\mu\text{L}\cdot\text{min}^{-1}$ (R1: 114 ± 11 bar, R2: 98 ± 9 bar; approx. 18 s residence time), injection time was 2 s each. Column: Chiralpak IG-3. Mobile phase: 75 $\mu\text{L}\cdot\text{min}^{-1}$, $\text{H}_2\text{O}:\text{MeCN}$ (55:45 vol% with 0.1 vol% FA; 98 ± 9 bar at pump, 45 ± 2 bar waste bypass R1). Pinch flow: 2 $\mu\text{L}\cdot\text{min}^{-1}$, $\text{H}_2\text{O}:\text{MeCN}$ (55:45 vol% with 0.1 vol% FA); **B)** Visualization of the monitored pressures for the connected pumps, as well as an external pressure sensor after the outlet channel of the first reactor. The eluent pump was connected to an active backpressure regulator for increased pressure stability.

3.4. 2R – PS/Si comparison in single chip

To compare the applicability of different solid supports for immobilized catalysts, a Ley-Arvidsson-Yamamoto catalyst immobilized on silica support was packed in the first reactor and an equivalent catalyst immobilized on polystyrene in the second reactor. Then, a Mannich reaction was conducted in both reactors and sampled alternately each 25 min as shown in Fig. S14 A (acquisitions from the reactor with polystyrene are shown in dotted lines). Since both reactors showed different backpressures while running at the same flow parameters (if operated single-handed), an internal standard was added due to different packing quality or solid support porosity. Subsequently, all acquired measurements were normalized according to the intensity of the internal standard, as shown in Fig. S14 B. Here, the catalyst immobilized on polystyrene showed significantly less product formation during the observed time range (as well as an increased remaining reactant signal). For better visibility of the product formation, the product signals are shown in Fig. S14 C with ten times multiplied intensity.

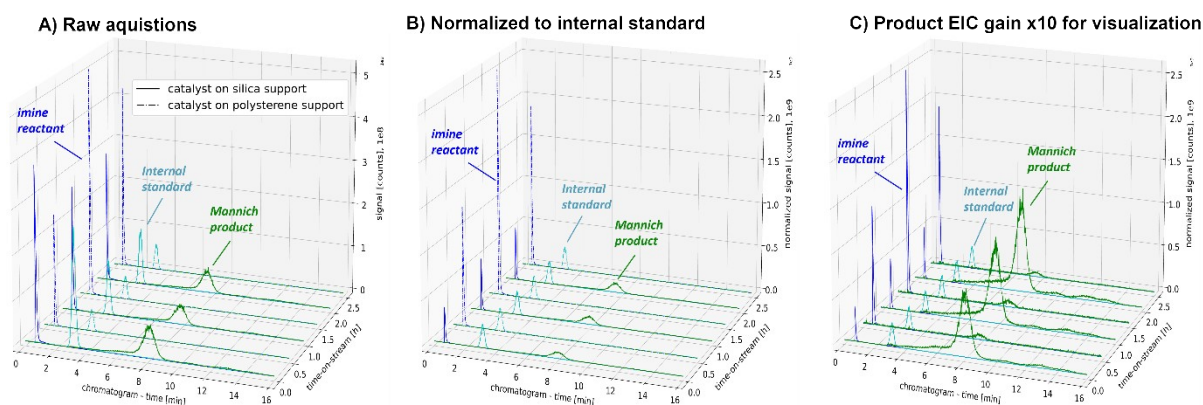


Fig. S14 Simultaneous screening of two Ley-Arvidsson-Yamamoto catalysts immobilized either on silica particles (data shown as solid lines; \varnothing 5 μm ; estimated loading $f = 0.76 \text{ mmol}\cdot\text{g}^{-1}$) or polystyrene resin (data shown as dashed lines; \varnothing 5 μm ; estimated loading $f = 0.32 \text{ mmol}\cdot\text{g}^{-1}$). The EICs for the reactant, internal standard, and products are shown. Both reactors: sample flow $0.5 \mu\text{L}\cdot\text{min}^{-1}$ (R1 101 ± 3 bar, R2 106 ± 2 bar; approx. 18 s residence time), injection time: 1 s. Column: Chiralpak IG-3. Mobile phase: $75 \mu\text{L}\cdot\text{min}^{-1}$, $\text{H}_2\text{O}:\text{MeCN}$ (55:45 vol% with 0.1 vol% FA; 69 ± 2 bar at pump, 56 ± 1 bar at R1 bypass outlet). Pinch flow: $2 \mu\text{L}\cdot\text{min}^{-1}$, $\text{H}_2\text{O}:\text{MeCN}$ (55:45 vol% with 0.1 vol% FA); **A**) raw acquisitions before normalization; **B**) Here, each measurement was normalized by the intensity of benzanilide as internal standard; **C**) Visualization of the product signals with tenfold intensities for better visibility.

Finally, since the applicability of the reactors on different solvents was tested in the previous section, also several solvents were tested for a microreactor packed with polystyrene. To prevent damage of the two-reactor chips, different solvents were tested only for a separate packed single-reactor chip (channel length: 1.9 cm, 150 μm width and 55 μm depth, resulting in a total volume of approx. 220 nl), coupled to an injection valve filled with the respective solvents. The compatibility of the tested solvents is shown in Fig. S15. Thereby, an operation with MeOH, MeCN, DMSO or the previously used eluent showed no problems, while an operation with apolar or chlorinated solvents led to either clogging or swelling of the microreactor. This could also lead to a deformation of the packed column, as shown in Fig. S15 (right).

solvent	microreactor PS compatibility
MeOH	
MeCN	
MeCN:H ₂ O – 50:50 0.1 % FA	
DMSO	
THF	Dissolving
Dioxane	Dissolving
CHCl ₃	Clogging
DCM	Clogging

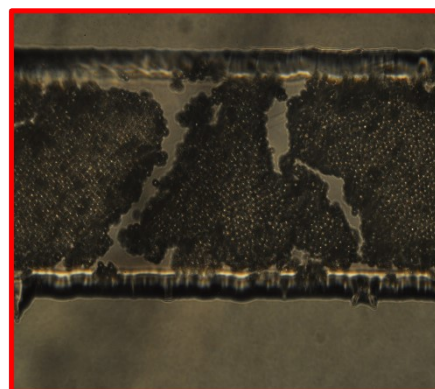
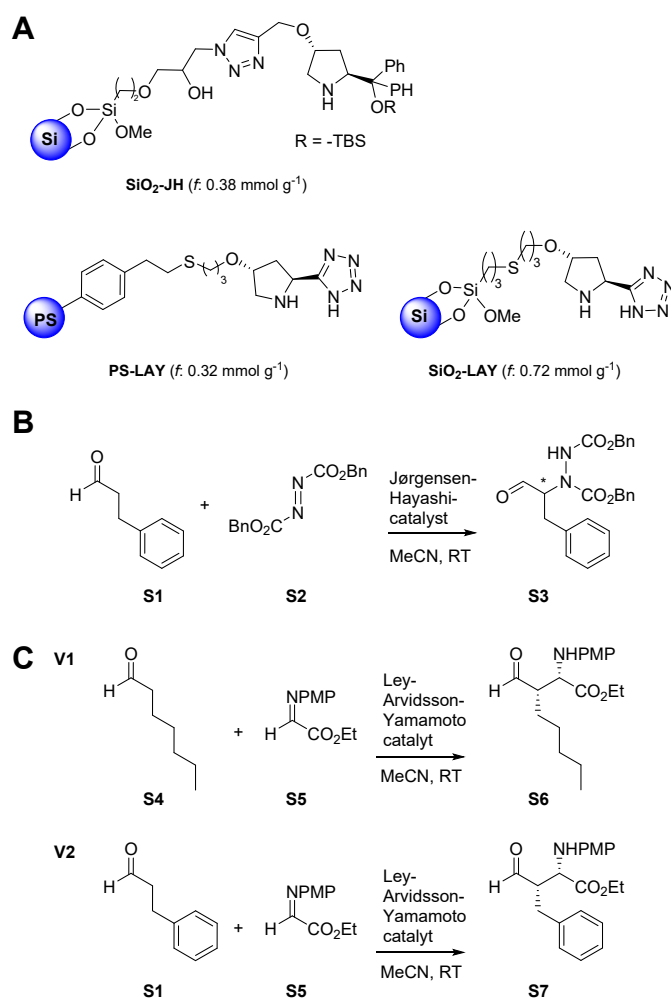


Fig. S15 Compatibility of the microreactor packed with polystyrene tested for different solvents. For this investigation a packed single-channel chip (1.9 cm long reactor) was used and coupled to an injection valve to introduce the respective solvents. A good compatibility is marked in green. On the right side a deformed column is depicted which resulted after using DCM as solvent in combination with a channel packed with polystyrene particles.

4. Continuous flow model reactions and peak identification

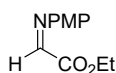
Continuous flow model reactions

For the microfluidic device, two model reactions were chosen for each of the two integrated reactors. In the first reactor, an α -amination was performed, where the reaction mixture consisted of 6.25 mM hydrocinnamaldehyde **S1**, 1.25 mM dibenzyl azodicarboxylate **S2**, and 0.625 mM CH₃COOH in MeCN, DCM or DMSO. For the second reactor, a Mannich-reaction was conducted consisting of 9.6 mM of either hydrocinnamaldehyde **S1** or heptanal **S4**, together with 1.0 mM N-PMP-ethyl-iminoglyoxylate **S5** in either MeCN, DCM, or DMSO. The microreactors were operated at room temperature and a flow rate of 0.5-1 $\mu\text{L}\cdot\text{min}^{-1}$, resulting in a residence time in the range of 9-18 s. The corresponding reaction schemes can be found under scheme S1.



Scheme S1: A) Organocatalysts immobilized on either silica or PS packed in the respective reactor channel. **B)** α -amination using hydrocinnamaldehyde as substrate and an immobilized Jørgensen-Hayashi catalyst. **C)** Mannich reaction using either heptanal or hydrocinnamaldehyde as substrate and an immobilized Ley-Arvidsson-Yamamoto catalyst.

Synthesis of N-PMP-ethyl-iminoglyoxylate **S5**



S5

p-Anisidine (5 g, 406 mmol) was dissolved in 40 mL of toluene in a 100 mL round bottom flask. Sodium sulfate (20 g, approx. 2.5 eq) was added while stirring. Ethyl glyoxylate (8.2 mL, 50% in toluene, 1 eq) was added slowly, and proper stirring was maintained. The reaction was completed in half an hour. After ensuring the absence of *p*-anisidine inside the reaction mixture, sodium sulfate was removed by filtration through a pad of celite, and toluene was removed under reduced pressure to yield the crude imine (8.2 g, 98% yield).

Signal assignment in α -amination reaction

The peak identification for the α -amination was performed by measuring the product's specific rotation compared to literature data, since no enantiomerically pure standard was available. According to the literature, the measured specific rotation in CHCl_3 of $[\alpha] = -16.7$ can be referred to the respective *S*-enantiomer.^[3]

Signal assignment in Mannich reaction

To identify the peaks of the *syn*-products, the reaction was conducted in batch with (*S*)- and (*R*)-proline as catalytic species (12 h reaction time, 2 mM proline each) and subsequently analyzed by chiral HPLC/MS (IG-3, Daicel). Additionally, the resulting signals were compared to the mass trace from the batch reaction catalyzed by the immobilized Ley-Arvidsson-Yamamoto catalyst.

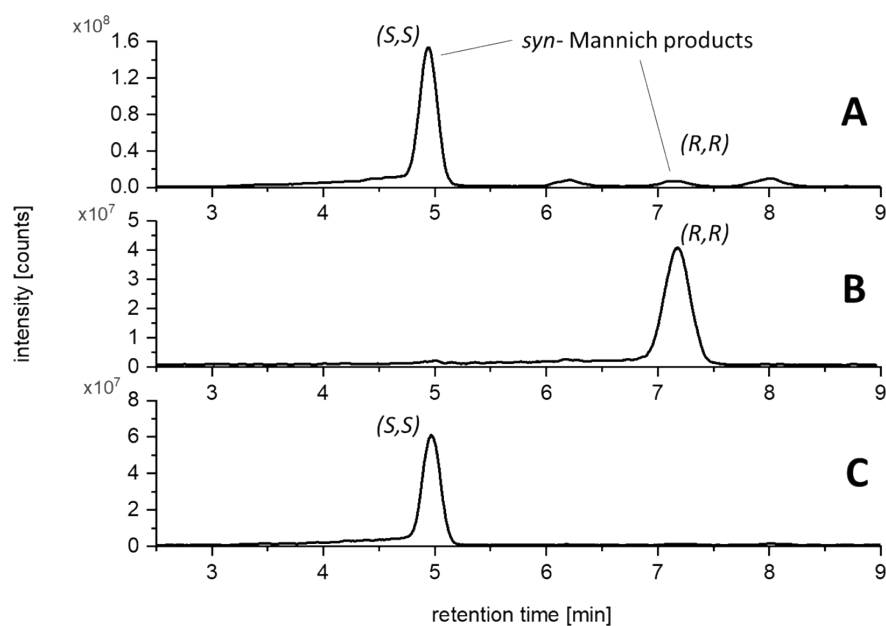
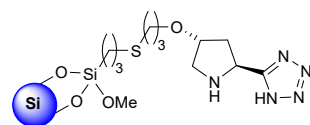


Figure S16. Identification of the product signals after the Mannich reaction of hydrocinnamaldehyde with the iminoglyoxylate **S1** under batch conditions (2 h reaction time, 10 mol% proline each). Analysis by conventional, chiral HPLC/MS (IG-3, 60:40 MeCN:H₂O, 0.1% formic acid, 500 $\mu\text{L}\cdot\text{min}^{-1}$). The extracted ion chromatograms for the product mass trace 342 m/z are depicted. **A**) – catalyzed by the immobilized Ley-Arvidsson catalyst (**LAY-Cat.**) **B**) – catalyzed by (*R*)-proline. **C**) – catalyzed by (*S*)-proline

5. Syntheses and immobilization of the organocatalysts

Ley-Arvidsson-Yamamoto-Catalyst (LAY-Cat.) on silica

The on silica immobilized catalyst was synthesized by thermal/photoinduced thiol-ene coupling, starting from mercaptopropyl silica gel (5 μm , 60 Å, Sigma Aldrich), as described in more detail in previous publications.^[1,4]



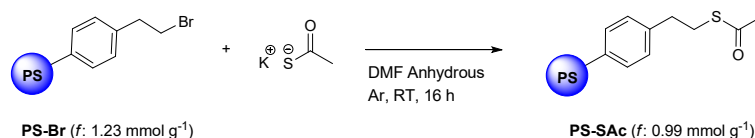
SiO₂-LAY (*f*: 0.72 mmol g⁻¹)

FT-IR (KBr): ν 2938, 1674, 1445 cm⁻¹.^[4]

CHN analysis (N): 5.32% (calculated loading $f = 0.76 \text{ mmol} \cdot \text{g}^{-1}$).^[4]

Ley-Arvidsson-Yamamoto-Catalyst (LAY-Cat.) on polystyrene (PS-LAY)

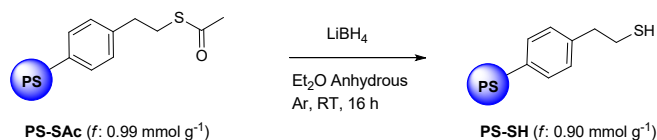
Preparation of mercaptoethyl polystyrene microspheres PS-SH



PS-Br resin (0.50 g, 0.61 mmol, $f = 1.23 \text{ mmol g}^{-1}$, 5 μm particle size, purchased by Rapp Polymere, prod. HM1501) was treated with potassium thioacetate (212 mg, 1.86 mmol) in anhydrous DMF (3.0 mL) and stirred at room temperature overnight. The mixture was next centrifuged (1200 rpm, 10 min) and suspended in THF (10 mL), stirred for 10 min and centrifuged again, removing the liquid phase. Same treatment was done with H₂O (10 mL) and THF (10 mL, 2 \times). The resulting resin **PS-SAc** was finally dried under reduced pressure (0.1 mbar, 40 °C, 16 h).

FT-IR (KBr): ν 3450, 2968, 1620, 1383, 1087 cm⁻¹.

CHN analysis (S): 3.18% (calculated loading $f = 0.99 \text{ mmol} \cdot \text{g}^{-1}$).

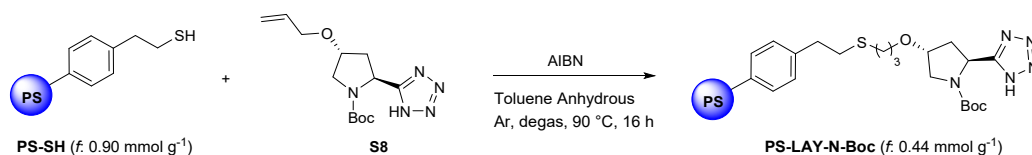


PS-SAc resin (400 mg, 0.4 mmol, $f = 0.99 \text{ mmol g}^{-1}$) was suspended in anhydrous Et₂O (3 mL), treated with a 2.0 M solution of LiBH₄ in THF (1.0 mL, 1.96 mmol) and stirred at room temperature overnight. The mixture was next centrifuged (1200 rpm, 10 min), suspended in H₂O (10 mL), stirred for 10 min and centrifuged again, removing the liquid phase. Same treatment was done with Et₂O (10 mL, 2 \times). The resulting resin **PS-SH** was finally dried under reduced pressure (0.1 mbar, 40 °C, 16 h).

FT-IR (KBr): ν 3453, 2931, 1620, 1394, 1105 cm^{-1} .

CHN analysis (S): 2.88% (calculated loading $f = 0.90 \text{ mmol}\cdot\text{g}^{-1}$).

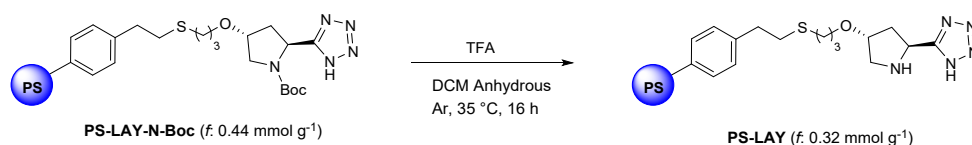
LAY Catalyst immobilization (PS-LAY): thermal thiol-ene coupling and Boc deprotection



A mixture of **PS-SH** (330 mg, 0.3 mmol; $f = 0.90 \text{ mmol}\cdot\text{g}^{-1}$), (4-allyloxy)pyrrolidine derivative **S8**^[4] (266 mg, 0.9 mmol), 2,2'-azobis(2-methylpropionitrile)(AIBN, 50 mg, 0.3 mmol), and anhydrous toluene (3.0 mL) was degassed under vacuum, and saturated with argon (by an Ar-filled balloon) three times. The mixture was then warmed to 90 °C, stirred for 16 h at the same temperature, cooled to room temperature, diluted with toluene (10 mL), and centrifuged with 10 mL portions of toluene and THF (2 \times). The resulting N-Boc protected Polystyrene-supported LAY catalyst **PS-LAY-N-Boc** was finally dried at reduced pressure (0.1 mbar, 40 °C, 16 h). Unreacted pyrrolidine derivative **S8** can be easily recycled by column chromatography of the centrifugate.

FT-IR (KBr): ν 3060, 2923, 1092, 1870, 1802, 1705, 1602, 1584 cm^{-1} .

CHN analysis (N): 3.09% (calculated loading $f = 0.44 \text{ mmol}\cdot\text{g}^{-1}$).

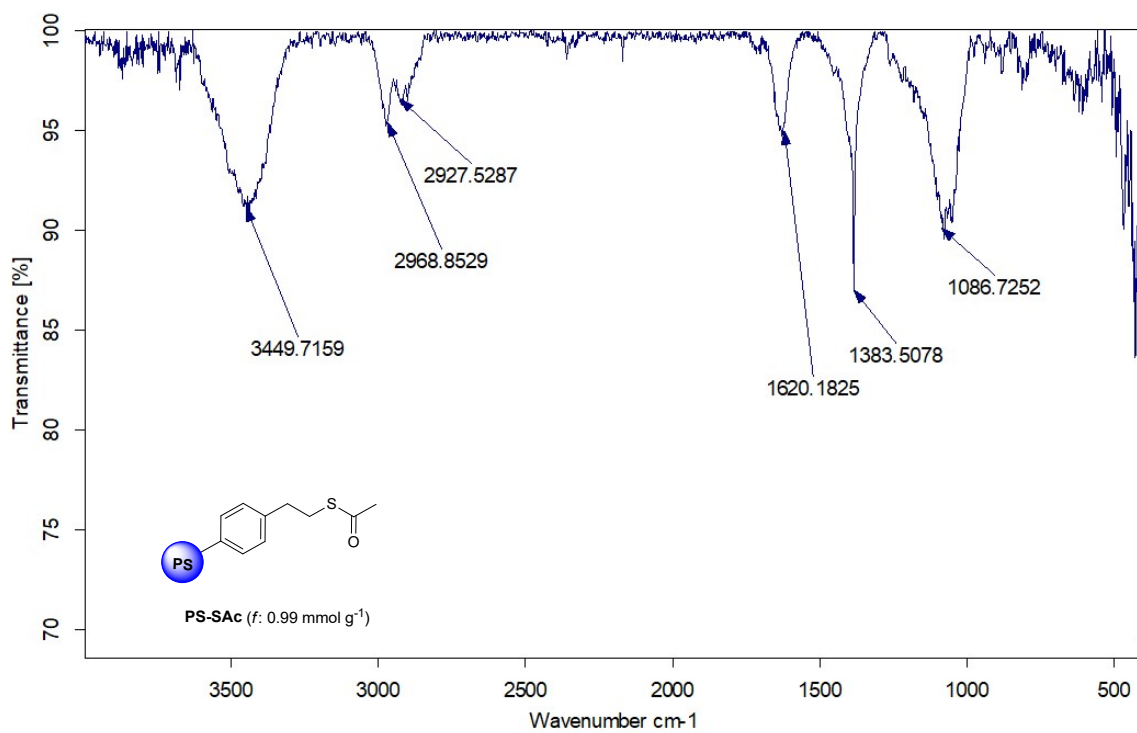


To a stirred mixture of **PS-LAY-N-Boc** resin (280 mg, 0.12 mmol, $f = 0.44 \text{ mmol}\cdot\text{g}^{-1}$) in DCM (3.0 mL), TFA (3.0 mL) was slowly added. The mixture was then warmed to 35 °C, stirred for 16 h, and centrifuged with 10 mL of DCM. After solvent removal, the resin was suspended in Et₃N-DCM 1 : 2 (2 \times ; addition at 0 °C), stirred for 30 min and centrifuged. Washing with 10 mL portions of MeOH (2 \times) and centrifugation afforded resin **PS-LAY** which was finally dried at a reduced pressure (0.1 mbar, 40 °C, 16 h). Disappearance of FT-IR Boc signal (1705 cm^{-1}) confirmed the successful deprotection.

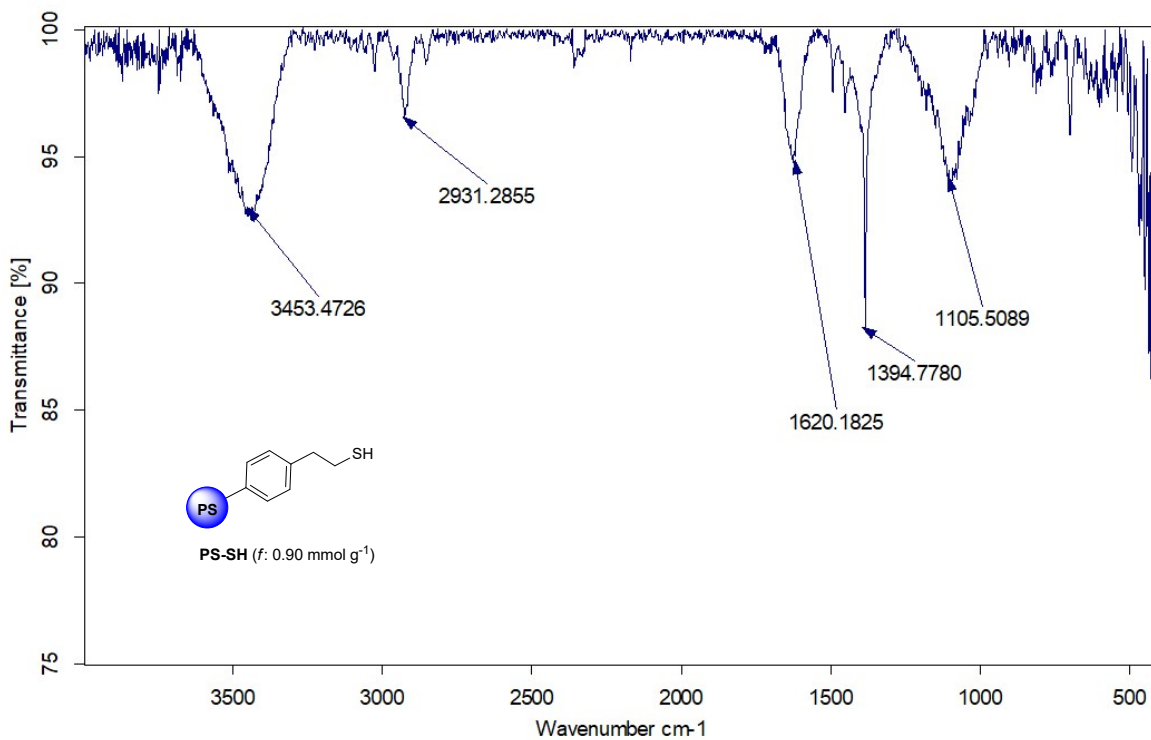
FT-IR (KBr): ν 3026, 2924, 1092, 1944, 1872, 1682, 1601, 1492, 1451 cm^{-1} .

CHN analysis (N): 2.28% (calculated loading $f = 0.32 \text{ mmol}\cdot\text{g}^{-1}$).

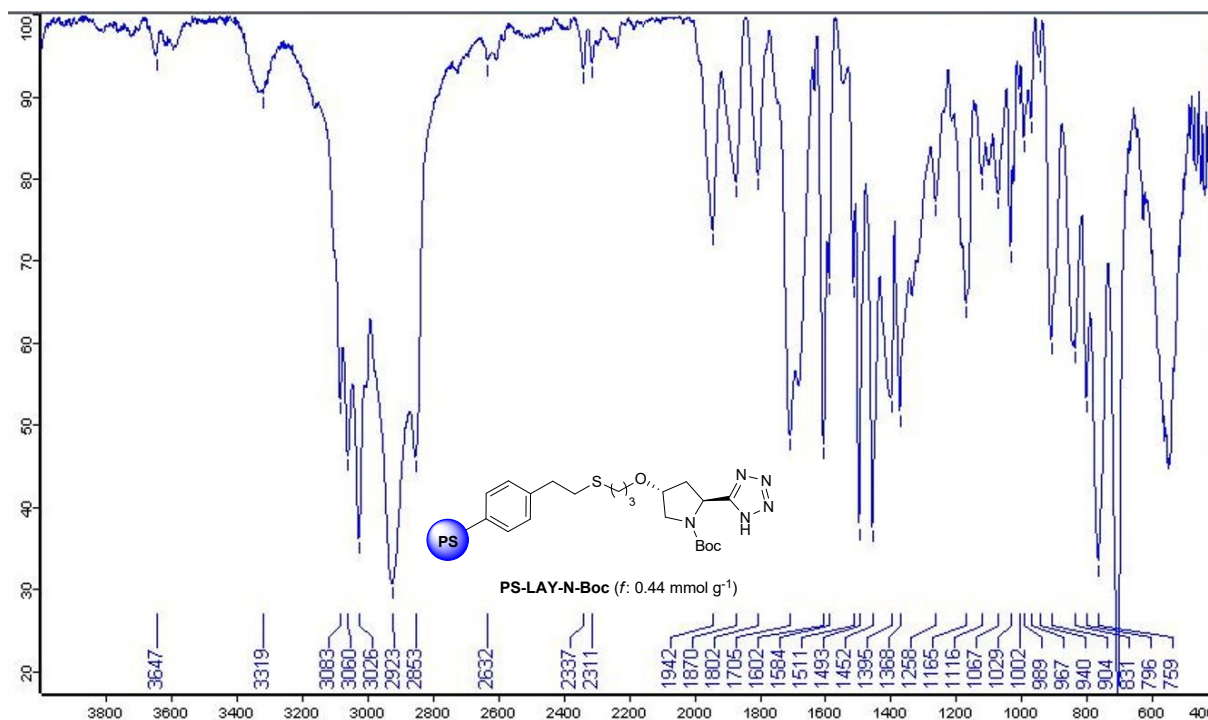
FT-IR spectra of PS-SAc



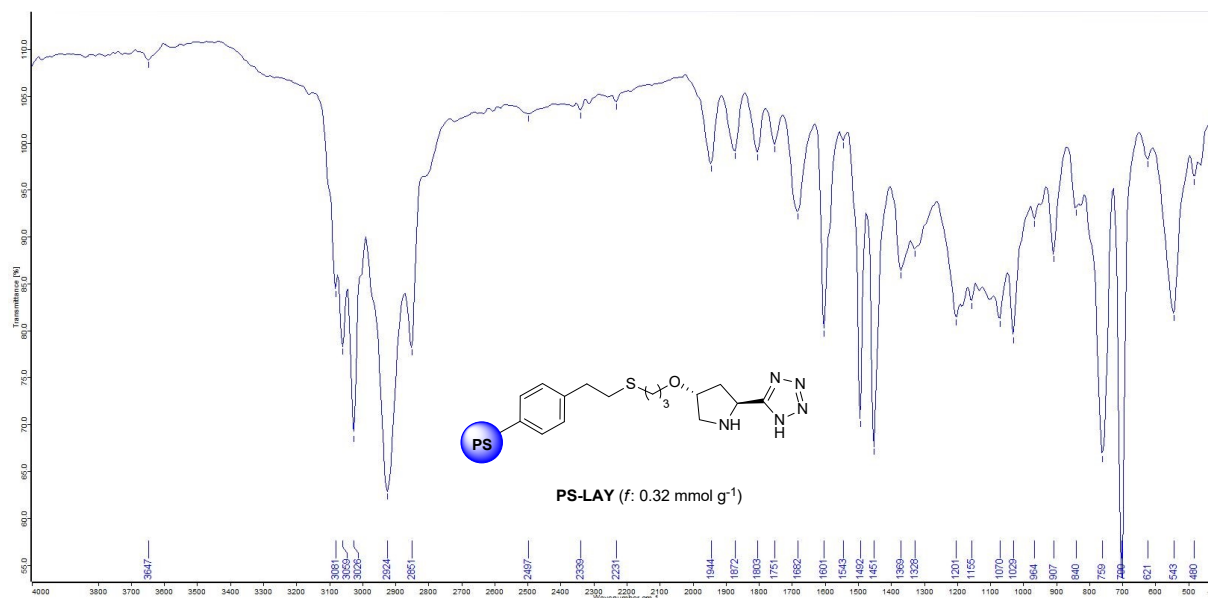
FT-IR spectra of PS-SH



FT-IR spectra of PS-LAY-N-Boc

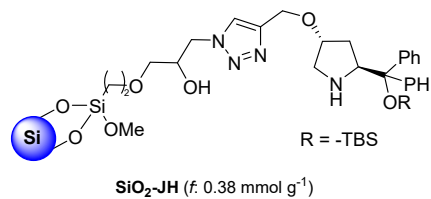


FT-IR spectra of PS-LAY



Jørgensen-Hayashi-Catalyst (JH-Cat.) on silica

The Jørgensen-Hayashi catalyst was synthesized with a *tert*-butyl dimethylsilyl group (TBS) protection group. Afterward, the catalyst was immobilized onto commercially available azide-functionalized porous silica particles by click chemistry via a copper(I)-catalyzed alkyne-azide cycloaddition (Kromasil, 5 μ m, 60 \AA , estimated loading $f = 0.38 \text{ mmol} \cdot \text{g}^{-1}$). A detailed description of the synthetic method can be found elsewhere.^[1,5,6]



References

- [1] H. Westphal, R. Warias, H. Becker, M. Spanka, D. Ragno, R. Gläser, C. Schneider, A. Massi, D. Belder, *ChemCatChem* **2021**, cctc.202101148.
- [2] C. Lotter, J. J. Heiland, V. Stein, M. Klimkait, M. Queisser, D. Belder, *Anal. Chem.* **2016**, *88*, 7481–7486.
- [3] C. Beattie, M. North, P. Villuendas, *Molecules* **2011**, *16*, 3420–3432.
- [4] O. Bortolini, L. Caciolli, A. Cavazzini, V. Costa, R. Greco, A. Massi, L. Pasti, *Green Chem.* **2012**, *14*, 992–1000.
- [5] L. Moni, A. Ciogli, I. D'Acquarica, A. Dondoni, F. Gasparri, A. Marra, *Chem. – Eur. J.* **2010**, *16*, 5712–5722.
- [6] I. Mager, K. Zeitler, *Org. Lett.* **2010**, *12*, 1480–1483.